A pressure-based numerical method for the simulation of compressible two-phase flow.

M. Boger*, F. Jaegle, S. Fechter, C.-D. Munz
Institute of Aerodynamics and Gas Dynamics, University of Stuttgart, Germany
{boger,jaegle,fechter,munz}@iag.uni-stuttgart.de

Abstract

In this contribution we present a pressure-based numerical scheme for the direct numerical simulation of two-phase flows. While for many technical applications, two-phase flows can be treated as incompressible, this assumption fails in cases with high pressure and temperature like they can be found in rocket combustion chambers, for example. Our interest is in the development of a pressure-based method that aims at the extension of an incompressible two-phase code to the compressible regime. The development builds upon a method that has originally been designed for single-phase flows. Its adaptation to three-dimensional (3D) two-phase flows is shown. This includes the possibility to resolve and track the interface as well as the description of the two phases by different equations of state. Furthermore, it is shown that the scheme does not necessitate a cumbersome interface treatment in three dimensions in order to avoid spurious oscillations in the vicinity of the material interface. Numerical examples of shock-droplet interactions are shown and our scheme proves to excellently simulate the propagation of shock waves in gaseous and liquid phases, including multiple wave reflections.

Introduction

Direct numerical simulation (DNS) of two-phase flows including the resolution of the material interface is usually performed with the incompressible Navier-Stokes equations. Typical technical applications concern droplets in an air environment at ambient pressure. In such a configuration, the liquid itself can be considered to be almost incompressible. Usually, the droplets are moving at low speed, such that the compressibility of the gas can also be neglected. Under these circumstances, kinetic and internal energy are decoupled resulting in the separation of thermodynamics and hydrodynamics, such that the assumption of an incompressible flow is justified. Yet, in the context of fuel injection processes, one has to face more extreme ambient conditions that are characterized by an augmented pressure and temperature. Especially for large pressure and temperature gradients in the flow field, compressible effects can be noticed and even be dominant. In such cases, the numerical simulation has to be based on the compressible flow equations in order to get accurate results.

The simulation of multiphase flows is always characterized by large jumps in the material properties across the interface separating two phases. An additional difficulty is the resolution and tracking of the interface itself. Both issues are of great importance for incompressible and compressible flows. However, the use of the compressible flow equations introduces different equations of state (EOS) on either side of the material interface. As the fluids can differ significantly in their properties, their EOS are also very different in nature. From a mathematical point of view, one has to deal with a stiff problem and the change in EOS is very challenging as it results quite often in spurious pressure and velocity oscillations in the vicinity of the interface, if there is no special remedy applied [1].

Our interest lies in the extension of an incompressible two-phase flow solver to the compressible regime. From a numerical point of view, the incompressible flow equations are solved by the so-called pressure-based schemes while the simulation of compressible flows is usually performed with density-based methods. Yet, there are several possibilities to extend an originally incompressible pressure-based method to the compressible flow equations. One of these approaches builds upon an asymptotic pressure decomposition, introducing multiple pressure variables that consider the different roles of pressure for compressible and incompressible flows. This scheme is called the Multiple Pressure Variables (MPV) method [2]. Its conservative formulation [3] is the basis of the numerical scheme that is described in this paper. The MPV method has been derived for single-phase flows [2, 3] and extended to the treatment of compressible two-phase flows in one space dimension [4]. In this paper we now present its extension to three space dimensions including its validation with the simulation of two 3D shock-droplet interactions.

The outline of the paper is as follows. In the first section, the governing equations are presented. Afterwards the MPV method and its extension to the treatment of 3D multiphase flows are described. This is followed by the presentation and discussion of the simulation of two shock-droplet interactions. The paper closes with a short conclusion and a perspective on future work.

*Corresponding author: boger@iag.uni-stuttgart.de

Governing Equations

This section gives an overview over the equations that build the basis of our numerical scheme.

Compressible Euler Equations

We use the 3D conservation equations for mass, momentum and total energy for inviscid flows without gravitational and external forces and heat conduction in compressible gas dynamics that are known as the Euler equations

$$\frac{\partial \rho'}{\partial t'} + \nabla \cdot (\rho' \mathbf{v}') = 0\,, \tag{1}$$

$$\frac{\partial (\rho' \mathbf{v}')}{\partial t'} + \nabla \cdot [(\rho' \mathbf{v}') \circ \mathbf{v}'] + \nabla p' = 0\,, \tag{2}$$

$$\frac{\partial e'}{\partial t'} + \nabla \cdot [\mathbf{v}' \, (e' + p')] = 0\,. \tag{3}$$

Here, ρ' denotes the density, p' the pressure, $\mathbf{v}'$ the velocity and e' the total energy per unit volume. Dimensional variables are marked by the superscript $'$. The system (1)-(3) has to be closed with an EOS relating the pressure to the known flow variables. A well-known formulation for gaseous fluids is the ideal gas EOS

$$p' = (\gamma - 1)(e' - \frac{\rho'}{2} \left|\mathbf{v}'\right|^2), \tag{4}$$

with γ being the adiabatic exponent. For liquids like water, the Tait EOS is used

$$p' = (\gamma - 1)(e' - \frac{\rho'}{2} \left|\mathbf{v}'\right|^2) - \gamma(k_0 - p_0). \tag{5}$$

Here, p_0 and k_0 are constants where the latter determines the compressibility of the fluid. However, there also exists the so-called stiffened gas EOS [5] that combines both previous EOS and that is used in the following

$$p = (\gamma - 1)(e' - \frac{\rho'}{2} \left|\mathbf{v}'\right|^2) - \gamma p_\infty. \tag{6}$$

The constant p_∞ characterizes the compressibility of the fluid. It is obvious that (6) includes the ideal gas EOS (4) by choosing $p_\infty = 0$ as well as the Tait fluid EOS (5) for $p_\infty = (k_0 - p_0)$.

The numerical scheme is based on the Euler equations in a dimensionless form and the following set of non-dimensional variables is introduced:

$$x = \frac{x'}{x_{ref}}, \quad \rho = \frac{\rho'}{\rho_{ref}}, \quad v = \frac{\mathbf{v}'}{|\mathbf{v}_{ref}|}, \quad p = \frac{p'}{p_{ref}}, \quad t = \frac{t' \, |\mathbf{v}_{ref}|}{x_{ref}}, \tag{7}$$

where the subscript *ref* denotes the reference values.

The pressure-based numerical method uses an asymptotic expansion of the pressure, such that the limit case of an incompressible flow is accessible. The speed of sound and the fluid velocity are given different reference values. This leads us to the introduction of a parameter called global flow Mach number M

$$M = \frac{|\mathbf{v}_{ref}|}{\sqrt{p_{ref}/\rho_{ref}}}, \tag{8}$$

that determines the compressibility of the flow. Using this set of variables the Euler equations (1)-(3) can be non-dimensionalized in the following way

$$\frac{\partial \rho}{\partial t} + \nabla \cdot (\rho \mathbf{v}) = 0\,, \tag{9}$$

$$\frac{\partial (\rho \mathbf{v})}{\partial t} + \nabla \cdot [(\rho \mathbf{v}) \circ \mathbf{v}] + \frac{1}{M^2} \nabla p = 0\,, \tag{10}$$

$$\frac{\partial e}{\partial t} + \nabla \cdot \left[\left(e + M^2 p\right) \mathbf{v}\right] = 0\,. \tag{11}$$

Level Set Method for Interface Tracking

For the DNS of two-phase flows, the interface location is of crucial interest. Therefore, an additional transport equation is introduced to describe the movement of the material interface between the two fluids. Based on [6], a level set variable Φ is initialized as a signed distance function with respect to the interface. Hence, its zero level set determines the interface position. In order to track the interface movement, the following transport equation in primitive variables can be used

$$\frac{\partial \Phi}{\partial t} + \mathbf{v}\nabla\Phi = 0. \tag{12}$$

To treat the level set function in a conservative manner, (12) is modified in the following way

$$\frac{\partial \Phi}{\partial t} + \nabla \cdot (\mathbf{v}\Phi) = \Phi \nabla \cdot (\mathbf{v}). \tag{13}$$

It is obvious that a new term appears on the right-hand side of the equation that has to be included as a source term.

The pressure-based Multiple Pressure Variables (MPV) method

The MPV scheme is a pressure-based method for the simulation of the compressible as well as the incompressible Euler equations. To avoid the singularity in the momentum equation (10) for the incompressible limit $M = 0$, caused by the term $1/M^2\nabla p$, the MPV scheme splits the pressure into multiple pressure variables

$$p(x,t) = p^{(0)}(t) + M^2 p^{(2)}(x,t). \tag{14}$$

The leading order pressure term $p^{(0)}$ satisfies the EOS in the limit case $M = 0$ and it is therefore called thermodynamic background pressure. The spatially and temporally variable pressure $p^{(2)}$ can be considered to be a hydrodynamic pressure as it guarantees the divergence-free condition for incompressible flows at $M = 0$. Due to the pressure splitting, the term $1/M^2\nabla p$ in equation (10) remains bounded in the incompressible limit and simply reduces to $\nabla p^{(2)}$.

Time Discretization

Combining compressible and incompressible flows, the MPV approach builds upon a semi-implicit time discretization. This includes an explicit discretization of the convection terms while all terms linked to the speed of sound are discretized implicitly. Inserting the stiffened gas EOS (6) and the pressure decomposition (14) into the non-dimensional Euler equations (9)-(11) we arrive at the following system

$$\begin{pmatrix} \rho \\ \rho\mathbf{v} \\ p + \gamma p_\infty + (\gamma-1)M^2 e_k \end{pmatrix}_t + \nabla \cdot \begin{pmatrix} \rho\mathbf{v} \\ (\rho\mathbf{v}) \circ \mathbf{v} \\ (\gamma-1)M^2 e_k \mathbf{v} \end{pmatrix}^{ex} + \nabla \cdot \begin{pmatrix} 0 \\ p^{(2)}\mathbf{I} \\ \gamma(p+p_\infty)\mathbf{v} \end{pmatrix}^{im} = \begin{pmatrix} 0 \\ 0 \\ 0 \end{pmatrix}. \tag{15}$$

The superscripts ex and im designate the explicit and implicit time discretization of the respective terms and $\mathbf{I}$ stands for the unity matrix. This procedure takes care of the physical and mathematical background. While the compressible Euler equations build a system of hyperbolic equations, the incompressible limit is described by a hyperbolic-elliptic system. Hence, pressure waves are traveling at infinite speed, the role of pressure in the Euler equations changes and requires an implicit treatment of the pressure terms. The semi-implicit discretization (15) clearly indicates that the density is treated independently in a fully explicit manner while momentum and energy equation contain explicit as well as implicit parts.

As it is common for incompressible projection methods, the MPV scheme finally is based on the solution of a Poisson equation derived by introducing the following predictor-corrector relations for pressure and velocity:

$$p^{(2)n+1} = p^{(2)*} + \delta p^{(2)}, \tag{16}$$

$$\mathbf{v}^{n+1} = \mathbf{v}^* + \delta\mathbf{v}. \tag{17}$$

The δ designates the corrector value for the corresponding predictor that is marked by the superscript $*$ and the superscript $n+1$ stands for the new time level. Starting with the pressure $p^{(2)n}$ at the old time level as a guess

for the predictor $p^{(2)*}$, the velocity $\mathbf{v}^*$ follows directly from the momentum equation.
In the following, the equations are discretized in time such that a semi-discrete formulation is obtained (still continuous in space but discrete in time). This approach is known as the method of lines where a partial differential equation (PDE) is transformed into an ordinary differential equation (ODE) by the choice of a spatial discretization. Afterwards, the resulting ODE can then be solved by an appropriate time discretization scheme. At present, we use two different time discretizations that are of first and second order accuracy. In general, the ODE that results from the semi-implicit MPV approach can be written as follows

$$\frac{d\mathbf{U}}{dt} = \mathbf{f}(\mathbf{U}^n) + \mathbf{g}(\mathbf{U}^{n+1}), \tag{18}$$

where $\mathbf{U}$ designates the vector of the discretized conservative variables of the Euler equations and Δt stands for the discrete time step. The operator $\mathbf{f}(\mathbf{U^n})$ represents the explicitly discretized, non-stiff convective terms while the stiff terms are discretized implicitly and grouped together in the operator $\mathbf{g}(\mathbf{U^{n+1}})$.
The first order scheme uses the simple explicit and implicit Euler method that can be expressed as follows

$$\mathbf{U}^{n+1} = \mathbf{U}^n + \Delta t \left[\mathbf{f}(\mathbf{U}^n) + \mathbf{g}(\mathbf{U}^{n+1})\right]. \tag{19}$$

To achieve a second order temporal discretization method, we use a combination of Runge-Kutta for the explicit part and Crank-Nicolson (RK2CN) for the implicit terms of the MPV approach. This approach necessitates the introduction of a half time level

$$\mathbf{U}^{n+1/2} = \mathbf{U}^n + \frac{\Delta t}{2}\left[\mathbf{f}(\mathbf{U}^n) + \mathbf{g}(\mathbf{U}^{n+1/2})\right], \tag{20}$$

$$\mathbf{U}^{n+1} = \mathbf{U}^n + \Delta t \mathbf{f}(\mathbf{U}^{n+1/2}) + \frac{\Delta t}{2}\left[\mathbf{g}(\mathbf{U}^n) + \mathbf{g}(\mathbf{U}^{n+1})\right]. \tag{21}$$

Based on the respective time discretization, a relation between the two correctors $\delta\mathbf{v}$ and $\delta p^{(2)}$ is obtained from the momentum equations. The Poisson equation for the pressure corrector $\delta p^{(2)}$ can be derived by introducing the correctors for pressure (16) and velocity (17) and their relation to each other into the energy equation of (15). A more detailed description of the numerical method can be found in [3, 4].

Space Discretization

The spatial discretization is carried out on a Cartesian, staggered grid in three space dimensions, according to [7]. For the purpose of explanation, such a mesh is depicted in Fig. 1 for the two-dimensional case. It is obvious, that there are different control volumes (CV) for mass and momentum. While all scalar values like density, pressure and the level set function are located at the cell center of the mass CV, the velocity components are stored at the center of the momentum CV that coincides with the center of the mass CV cell faces. The same principle is applied in three dimensions. The convective fluxes for the first order spatial discretization are evaluated in a simple upwind manner. For the second order version, a linear reconstruction is performed based on the MUSCL approach [8].

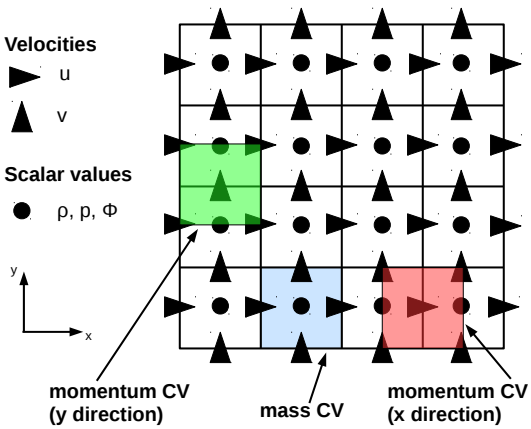

Figure 1. Staggered grid arrangement: overview over variables and different control volumes (CV).

Interface Tracking

The DNS of compressible two-phase flows is a rather challenging task as the two fluids often differ significantly in their material properties as well as in their thermodynamic behavior expressed by the EOS. For this

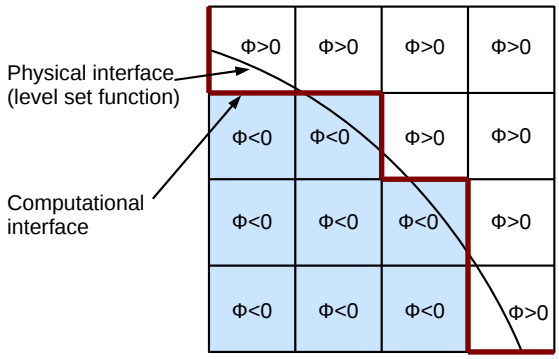

Figure 2. Physical and computational interface.

reason, it is crucial to accurately know and track the interface location at each time step. With the introduction of the level set function Φ and the corresponding transport equation (12), we are able to describe and evolve the material interface throughout the computation. The level set Φ is initialized as a signed distance function, such that its zero level set coincides with the interface location. Hence, we are able to easily assign the different fluids by the sign of the level set. While Φ has a positive sign in the gaseous phase, it is negative in the liquid phase.
Due to the use of the general stiffened gas EOS formulation (6) the MPV method offers the possibility to treat two different fluids distinguished by their values of the constants γ and p_∞. For the multiphase computation, both constants are allowed to vary from one grid cell to another such that each cell (i, j, k) is assigned to specific values $\gamma_{(i,j,k)}$ and $p_{\infty,(i,j,k)}$. At each time step, a loop over all grid cells is performed and based on the level set variable the corresponding values $\gamma_{(i,j,k)}$ and $p_{\infty,(i,j,k)}$ are set. This treatment shifts the physical interface to the cell faces, creating a computational interface that is of staircase shape, as it can be seen in Fig. 2. Once $\gamma_{(i,j,k)}$ and $p_{\infty,(i,j,k)}$ are assigned, the usual MPV solution procedure of the Poisson equation can be applied, taking into account the spatially variable constants.
The material interface represents a discontinuity in the EOS what may lead to spurious pressure and velocity oscillations at this location, especially when density-based flow solvers in conservative formulation are used without any special interface treatment [1]. We have already shown that our approach based on the conservative MPV method does not need any special interface treatment to prevent oscillations [4]. This is confirmed by the following numerical results.

Results

In the following, two numerical test cases are presented. Both of them are shock-droplet interactions. For both test cases we use the following setup, unless otherwise stated. The ideal gas EOS with $\gamma = 1.4$ is used for the surrounding gas phase and the stiffened gas EOS with $p_\infty = 3309$ for the liquid phase inside the droplet. The computations are carried out with the second order RK2CN MPV method and we use 64 grid cells in each of the three spatial directions.

Shock-droplet interaction: single droplet

The first test case describes the impact of an initially planar shock wave on a spherical droplet. The initial conditions of the test case are specified in Fig. 3 that also shows the pressure distribution on a slice through the center of the droplet at the instant $t = 4.25 \cdot 10^{-3}$. A more detailed analysis of the pressure field can be carried out by having a closer look at the distribution at different instants. For this purpose, the distributions of the pressure and the pressure gradient are given in Fig. 4. Plotting the gradient of the pressure, the wave structures can be resolved in more detail. When the shock wave is impinging on the droplet surface, the shock is reflected as well as transmitted into the droplet. While the reflected wave forms a bow shock due to the spherical geometry of the droplet, the transmitted wave is traveling through the droplet. Because of the higher speed of sound inside the droplet, the shock wave obviously is moving faster inside than outside the droplet. This is evident from the plot at $t_1 = 1.5 \cdot 10^{-3}$ in Fig. 4. The pressure distribution inside the droplet is no longer uniform indicating that the shock has already traveled through the complete droplet. Moreover, the shock is reflected at the rear part as an expansion

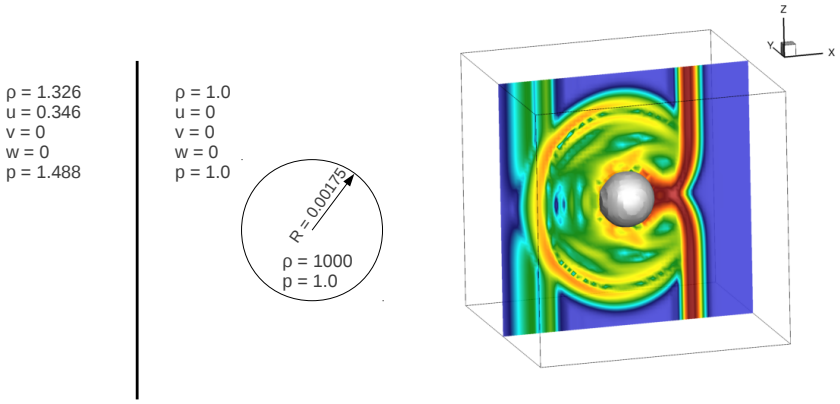

Figure 3. Sketch of the setup for the 3D shock-droplet interaction test case (left) and a slice through the droplet center at $t = 4.25 \cdot 10^{-3}$ showing the pressure gradient $\log(|\nabla p| + 1)$ (right).

that is moving back to the front. During the following time steps, the waves are reflected several times inside the droplet. At $t_2 = 4.25 \cdot 10^{-3}$, the shock wave has made its way around the droplet and the waves are interacting at the rear part, forming a curved shock front. Looking at the plots of pressure and pressure gradient, both are indicating a perfectly symmetric distribution. The MPV method with the above presented interface treatment is

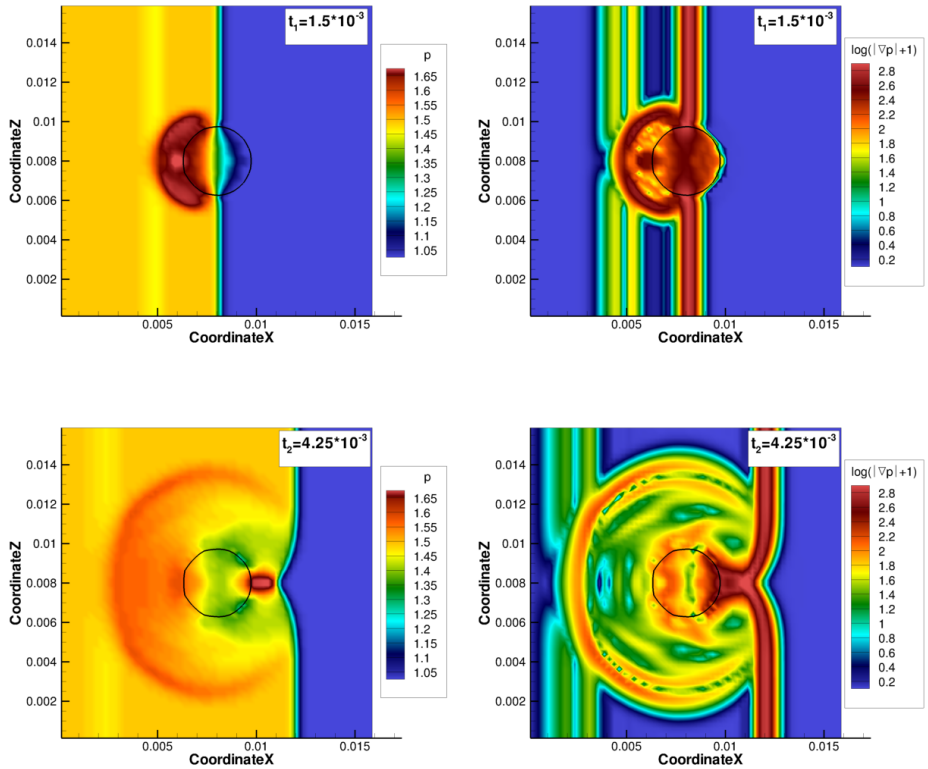

Figure 4. Pressure p and pressure gradient $\log(|\nabla p| + 1)$ at $t_1 = 1.5 \cdot 10^{-3}$ (top) and $t_2 = 4.25 \cdot 10^{-3}$ (bottom). 3D shock-droplet interaction test case, slices through the droplet center.

not suffering from any pressure or velocity oscillations near the interface. This is illustrated by Fig. 5. The contour lines of pressure show a smooth transition between the two phases. Additionally, the velocity vectors are not indicating any oscillations. Hence, the pressure-based MPV method proves to give oscillation-free results for the 3D simulation of compressible two-phase flows.

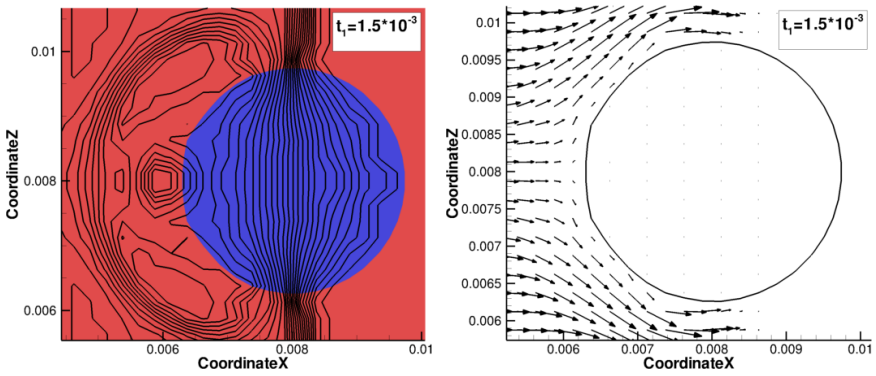

Figure 5. Contour lines of pressure (left) and velocity field with vectors at each grid node (right) for the 3D shock-droplet interaction test case. Slice through the droplet center at $t = 1.5 \cdot 10^{-3}$.

Shock-droplet interaction: two droplets

For this test case, a second spherical droplet is introduced. This generates additional wave reflections and interactions that finally result in a more complex wave pattern. The initial setup is presented in Fig. 6 as well as

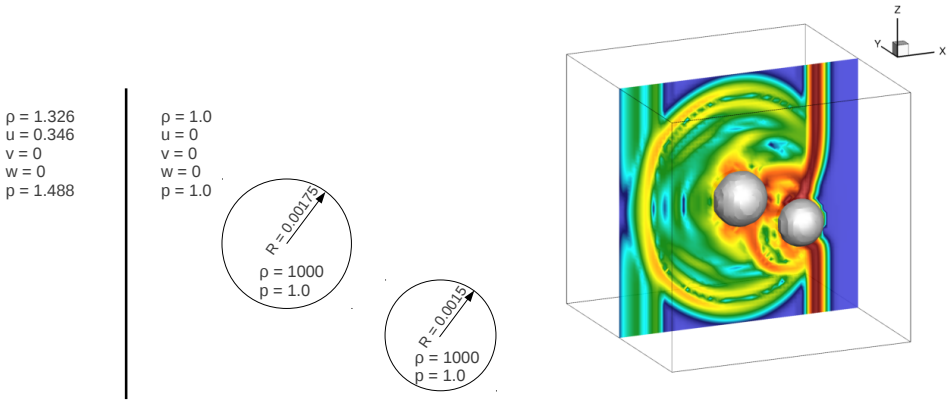

Figure 6. Sketch of the setup for the 3D shock-droplet interaction test case including two spherical droplets (left) and a slice through the droplet centers at $t = 5 \cdot 10^{-3}$ showing the pressure gradient $\log(|\nabla p| + 1)$ (right).

the pressure gradient distribution on a slice through the droplet centers. Similar to the single droplet case, Fig. 7

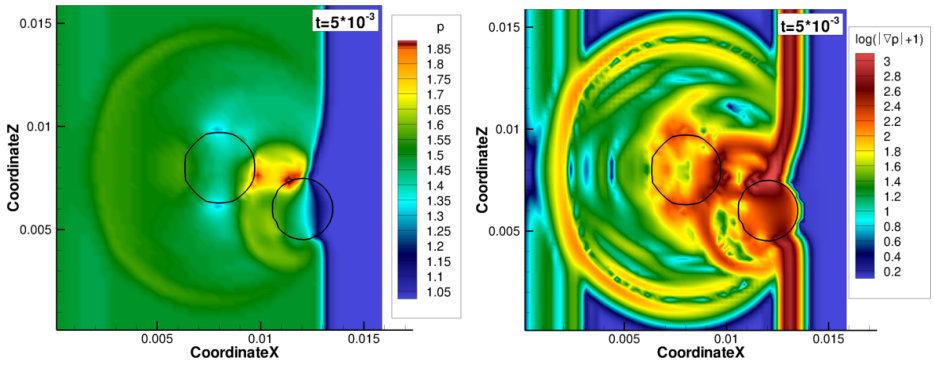

Figure 7. Pressure p and pressure gradient $\log(|\nabla p| + 1)$ at $t = 5 \cdot 10^{-3}$. Slices through the droplet centers.

illustrates the pressure as well as the pressure gradient distribution at the instant $t = 5 \cdot 10^{-3}$. It can be seen, that we have a non-symmetric pressure distribution inside the bigger droplet. This is due to the presence of the smaller droplet. The right moving initial shock wave finally impinges on the surface of the smaller droplet where it is

reflected. The reflected wave has a curved shape, it travels back towards the bigger droplet and hits its surface in the rear part. This impact influences the wave pattern inside the big droplet. In Fig. 8 we compare a 3D simulation

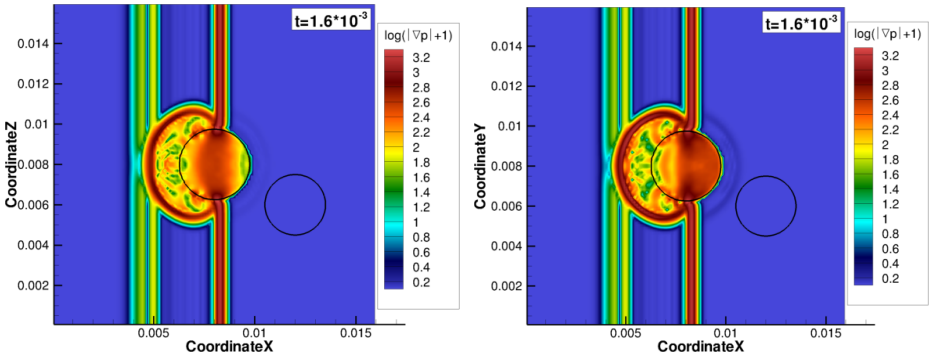

Figure 8. Pressure gradient $\log(|\nabla p| + 1)$ at $t = 1.6 \cdot 10^{-3}$ for the 3D (128^3 grid cells, slice through the droplet center; left) and the 2D (128^2 grid cells; right) calculation of the shock-droplet interaction with two droplets.

to a two-dimensional one at $t = 1.6 \cdot 10^{-3}$. There are two remarkable points. First of all, the wave patterns inside the droplets look different. This is due to 3D effects, caused by the spherical shape of the 3D droplet that causes differences in the wave reflections in comparison to the 2D case. Moreover, behind the bigger droplet, a very weak shock wave is visible. This wave is transmitted through the droplet. It is clearly more pronounced in the 2D case than in the 3D calculation.

Conclusions

In this paper a pressure-based numerical scheme for the simulation of 3D compressible two-phase flows is presented. The algorithm is based on an asymptotic pressure expansion. It can be used to extend originally incompressible multiphase methods to the compressible flow regime as it formally allows the simulation of incompressible as well as compressible flows. Unlike many other approaches for compressible two-phase flows that encounter spurious oscillations at the material interface, a cumbersome special interface treatment can be avoided. The physical interface is described by the zero level set function and it is shifted to the cell boundaries for the computations. Two multidimensional test cases are shown and the MPV method proves to resolve complex wave patterns including several wave reflections inside and outside of liquid droplets. The scope of the future work is directed to further enhance the tracking and the resolution of the interface. To be able to include additional physical phenomena such as surface tension, our aim is to use a more sophisticated interface tracking scheme. The present simple level set indicator will be replaced by a more elaborated level set method based on a discontinuous Galerkin (DG) scheme of high order. The polynomial representation of the level set function by the DG scheme allows to easily and accurately evaluate its derivative that is needed to determine surface normals and curvature. Furthermore, we plan to include viscous effects and to extend the numerical scheme to the compressible Navier-Stokes equations.

Acknowledgements

The authors would like to thank the German Research Foundation (DFG) for financial support of the project within the Cluster of Excellence in Simulation Technology (EXC 310/1) at the University of Stuttgart and the SFB-Transregio 40.

References

[1] Abgrall, R. and Karni, S., *Journal of Computational Physics* 169:594-623 (2001).
[2] Munz, C.-D., Roller, S., Klein, R. and Geratz, K.J., *Computers & Fluids* 32:173-196 (2003).
[3] Park, J.H. and Munz, C.-D., *International Journal for Numerical Methods in Fluids* 49:905-931 (2005).
[4] Boger, M., Jaegle, F. and Munz,C.-D. *Proc. 24th European Conference on Liquid Atomization and Spray Systems, Estoril, Portugal*, 2011.
[5] Saurel, R. and Abgrall, R., *SIAM Journal on Scientific Computing* 21(3):1115-1145 (1999).
[6] Osher, S. and Sethian, J. A., *Journal of Computational Physics* 79(1):12-49 (1988).
[7] Harlow, A. T. and Welch, J. E., *Physics of Fluids* 8:2182-2189 (1965).
[8] van Leer, B., *Journal of Computational Physics* 32:101-136 (1979).